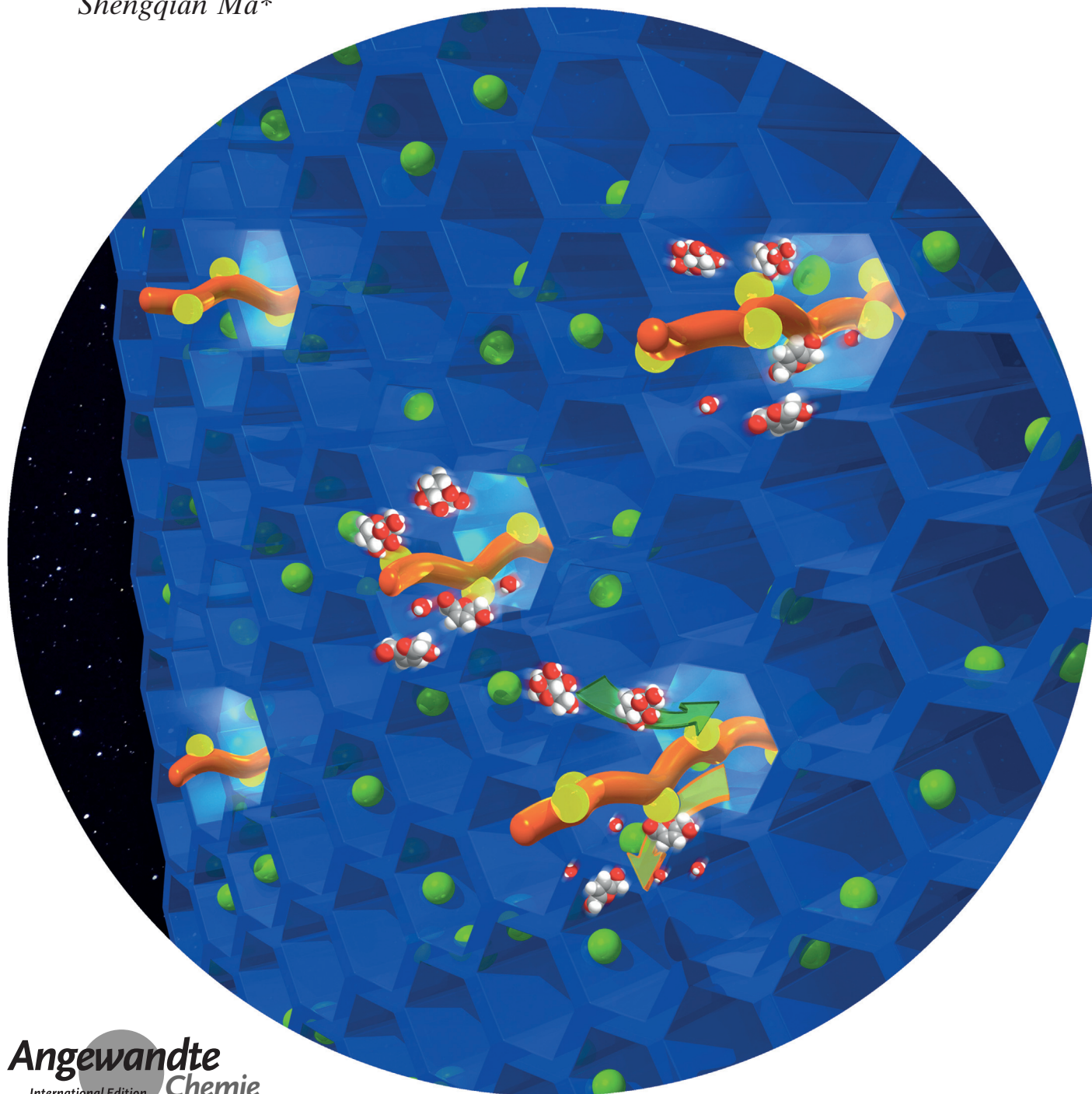


Covalent Organic Frameworks

International Edition: DOI: 10.1002/anie.201900029  
German Edition: DOI: 10.1002/ange.201900029

# Reaction Environment Modification in Covalent Organic Frameworks for Catalytic Performance Enhancement

Qi Sun<sup>+</sup>, Yongquan Tang<sup>+</sup>, Briana Aguila, Sai Wang, Feng-Shou Xiao,\*  
Praveen K. Thallapally, Abdullah M. Al-Enizi, Ayman Nafady, and  
Shengqian Ma\*



**Abstract:** Herein, we show how the spatial environment in the functional pores of covalent organic frameworks (COFs) can be manipulated in order to exert control in catalysis. The underlying mechanism of this strategy relies on the placement of linear polymers in the pore channels that are anchored with catalytic species, analogous to outer-sphere residue cooperativity within the active sites of enzymes. This approach benefits from the flexibility and enriched concentration of the functional moieties on the linear polymers, enabling the desired reaction environment in close proximity to the active sites, thereby impacting the reaction outcomes. Specifically, in the representative dehydration of fructose to produce 5-hydroxymethylfurfural, dramatic activity and selectivity improvements have been achieved for the active center of sulfonic acid groups in COFs after encapsulation of polymeric solvent analogues 1-methyl-2-pyrrolidinone and ionic liquid.

The functions of active sites are directly linked to the local environment where they are housed.<sup>[1]</sup> There is a growing body of evidence that the strategic placement of noncovalent interactions around a catalytic center can lead to remarkable increases in selectivity and activity by stabilizing the transition state and having favorable conformations of the active site and the products, in a way reminiscent of enzymatic catalysis.<sup>[2]</sup> Although profitable, precise control over the periphery of an active site remains synthetically challenging, particularly in heterogeneous catalytic systems.<sup>[3]</sup> Unlike in biological/molecular systems, difficulties arise in solid systems because their structures are often rigid, impeding the cooperation between different catalytic elements and thereby underscoring the need for new innovative technologies.

Covalent organic frameworks (COFs), a class of porous, crystalline materials, have quickly moved to the forefront of materials science due to their unprecedented combination of ready chemical tunability, high crystallinity, tunable pore

structure, large surface area, and stability.<sup>[4,5]</sup> In COFs it is possible to exert control over the nature of a catalytic center and its spatial organization as well as the identity and placement of surrounding surface functionalities, forming structurally well-defined active sites.<sup>[6]</sup> The ordered pore channels and large pore volumes of COFs make them very attractive as host materials for guest encapsulation.<sup>[7]</sup> The functional space within the pores of COFs thus provides an auspicious platform for integrating multiple components, allowing synergistic catalytic activation pathways to be triggered. Indeed, multifunctional heterogeneous catalysts based on host-guest cooperation have recently emerged as state-of-the-art hybrid materials to tailor and enhance properties far beyond that of the combined soluble parent species.<sup>[8]</sup> In that scenario, the catalytic moieties on the flexible linear polymer, which are enriched in the pore spaces, promote them to cooperate with the active sites anchored on the pore walls of the host materials, lending to exceptional performances, while providing the additional benefit of recycling. Given these, it was hypothesized that this strategy could be used to emulate some of the design principles of enzymes, for which the improved performances are reliant on both the highly potent catalytic center and the surrounding polypeptide chains, and thereby would allow access to new types of catalysts. In view of the high sensitivity of chemical reactions towards changes in the solvation environment, we encapsulated polymeric solvent analogues as a proof-of-principle study.<sup>[9]</sup> It is shown that the partnership with the catalytic elements on the COFs and the linear polymers hosted in the pore channels gives great promise to optimize the reaction outcomes (Figure 1). Specifically, the performance of sulfonic acid groups on COFs can be greatly amplified after the introduction of polymeric solvent analogues. The desired solvation environments are created by exerting hydrogen-bonding interactions to achieve activity and selectivity, as exemplified by the fructose to 5-hydroxymethylfurfural (HMF) transformation.

To implement this strategy, we first selected a COF prototype for the potential installation of catalytic elements as well as providing room for guest encapsulation. Earlier work has established that the COF, TPB-DMTP-COF, synthesized by the condensation of 1,3,5-tris(4-aminophenyl)benzene (TPB) and 2,5-dimethoxyterephthalaldehyde (DMTA), can be used as an excellent material platform for structural design and functional development, as well as for guest encapsulation due to its high crystallinity and large mesoporous channels, in conjugation with ultrastability towards a wide range of conditions including strong acids and strong bases.<sup>[10]</sup> By a multivariate (MTV) approach, followed by postsynthetic modification, a family of COF-based catalysts can be achieved, whereby the catalytic groups are appended in a predefined way. A diverse range of catalytic moieties is amenable to this role, for example organocatalysts, and here, we opted for the sulfonic acid group given its versatility for a variety of industrially relevant reactions.<sup>[11]</sup> The second aspect of our design strategy is the insertion of functional linear polymers into the pore channels. We anticipated that, via noncovalent interactions with the reaction participants, the hosted linear polymers may be

[\*] Dr. Q. Sun,<sup>[†]</sup> B. Aguila, Prof. S. Ma  
Department of Chemistry, University of South Florida  
4202 East Fowler Avenue, Tampa, FL 33620 (USA)  
E-mail: sqma@usf.edu

Y. Tang,<sup>[†]</sup> S. Wang, Prof. F.-S. Xiao  
Key Lab of Applied Chemistry of Zhejiang Province  
Zhejiang University  
Hangzhou 310007 (China)  
E-mail: fsxiao@zju.edu.cn

Dr. Q. Sun<sup>[†]</sup>  
College of Chemical and Biological Engineering  
Zhejiang University  
Hangzhou, 310027 (China)

Prof. P. K. Thallapally  
Physical and Computational Science Directorate  
Pacific Northwest National Laboratory  
Richland, WA 99352 (USA)

Prof. A. M. Al-Enizi, Prof. A. Nafady, Prof. S. Ma  
Chemistry Department, College of Science  
King Saud University  
Riyadh, 11451 (Saudi Arabia)

[†] These authors contributed equally to this work.

Supporting information and the ORCID identification number(s) for the author(s) of this article can be found under:  
<https://doi.org/10.1002/anie.201900029>.

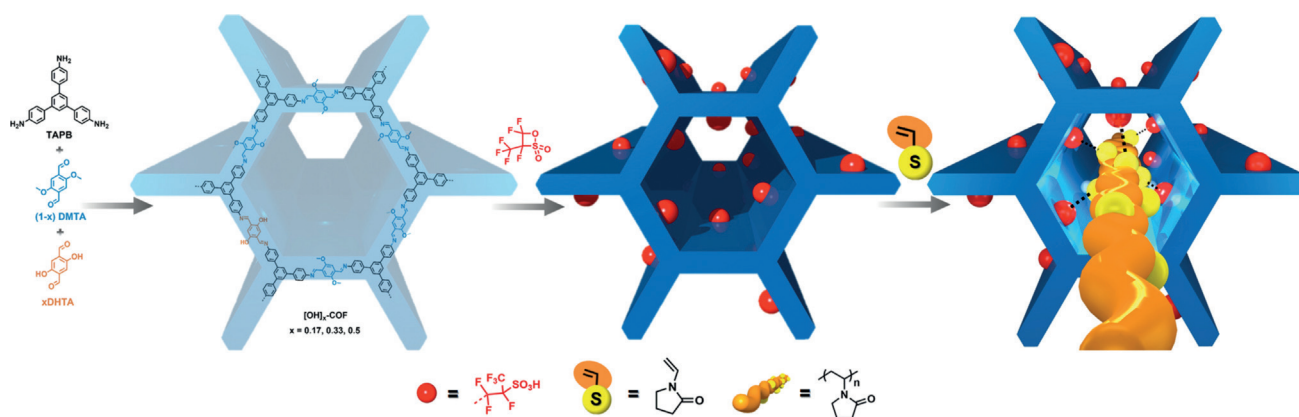


**Figure 1.** The concept of modification of the local reaction environment of the active sites on the porous materials by inserting highly flexible linear polymers, scheme for the synthesis of PVP@[SO<sub>3</sub>H]<sub>x</sub>-COF synthesis, and structures of [OH]<sub>x</sub>-COF ( $x = 0.17, 0.33, 0.5$ ).

able to influence the reaction rate or alter the activity and selectivity of product formation.

Our initial step was to introduce catalytically active perfluorinated sulfonic acid groups onto the pore walls of COFs. We employed a three-component condensation system with 2,5-dihydroxyterephthalaldehyde (DHTA) and 2,5-dimethoxyterephthalaldehyde (DMTA) as edge units to synthesize the intermediate [OH]<sub>x</sub>-TPB-DMTP-COFs (hereafter abbreviated as [OH]<sub>x</sub>-COF), where  $x$  is the percentage of functional groups as a fraction of the groups lining the pore walls. After treatment with 1,2,2-trifluoro-2-hydroxy-1-trifluoromethylethane sulfonic acid sultone, the perfluoroalkyl chains with terminal sulfonic acid functional groups were anchored onto the channel walls by the reaction between the sultone ring and OH group on the COFs, yielding [SO<sub>3</sub>H]<sub>x</sub>-COFs (Figure 1).

As representative samples, [OH]<sub>0.17</sub>-COF and the corresponding post-modified sample, [SO<sub>3</sub>H]<sub>0.17</sub>-COF, are described thoroughly here, whereas the detailed characterization results of other samples are provided in the Supporting Information. To examine the postsynthetic modification, we performed X-ray photoelectron spectroscopy (XPS), Fourier-transform infrared spectroscopy (FTIR), transmission electron microscopy energy-dispersive X-ray spectroscopy (TEM-EDX), and elemental analysis. The presence of the elements F (F 1s at 689.1 eV) and S (S 2p at 170.7 eV) signals in the XPS spectra of [SO<sub>3</sub>H]<sub>0.17</sub>-COF verified the occurrence of post-synthetic modification (Figure S1). Furthermore, additional peaks appeared at 1232 and 1445 cm<sup>-1</sup> in the IR spectrum of [SO<sub>3</sub>H]<sub>0.17</sub>-COF, corresponding to the C–F and S=O stretching vibrations, respectively, confirming the successful incorporation of perfluorinated sulfonic acid groups onto the COF (Figure S2).<sup>[12]</sup> The EDX mapping indicated the homogeneously distributed F, N, O, and S elements throughout the COF (Figure S3). To quantify the degree of post-synthetic modification, the content of S species in [SO<sub>3</sub>H]<sub>0.17</sub>-COF was evaluated by infrared absorption carbon–sulfur analysis, revealing that the content of sulfonic acid groups in the COF is 0.39 mmol g<sup>-1</sup> (Tables S1 and S2). To evaluate the acid strength of the resulting samples, we adsorbed trimethylphosphine oxide (TMPO) into [SO<sub>3</sub>H]<sub>0.17</sub>-COF and performed solid-state <sup>31</sup>P NMR spectroscopy. Given a linear

relationship between the <sup>31</sup>P chemical shift values of adsorbed TMPO and the strength of a Brønsted acid site, this technology has proven to be an informative tool for identifying the acidity of an acid site. A higher <sup>31</sup>P chemical shift corresponds to a stronger acid site due to the more polarized phosphorus–oxygen bond.<sup>[13]</sup> The <sup>31</sup>P MAS NMR spectrum of TMPO after interaction with [SO<sub>3</sub>H]<sub>0.17</sub>-COF gave a singlet peak at 76.0 ppm, indicating a moderate to high strength acidity (Figure S4). The narrow NMR signal suggests the homogeneity of the acid sites in these samples. The powder X-ray diffraction (PXRD) showed that the diffraction pattern of [SO<sub>3</sub>H]<sub>0.17</sub>-COF was in good agreement with that of [OH]<sub>0.17</sub>-COF (Figure 2a). N<sub>2</sub> sorption isotherms collected at 77 K revealed that [SO<sub>3</sub>H]<sub>0.17</sub>-COF and [OH]<sub>0.17</sub>-COF exhibited similar adsorption behavior, giving type IV isotherms. The BET surface area of [SO<sub>3</sub>H]<sub>0.17</sub>-COF was calculated to be 1510 m<sup>2</sup> g<sup>-1</sup>, slightly less than that of [OH]<sub>0.17</sub>-COF (1898 m<sup>2</sup> g<sup>-1</sup>, Figure 2b). Derived from nonlocal density functional theory modeling, both samples gave pore size distributions centered at 3.3 nm (Figure S5). These results confirmed that the postsynthetic modification had little effect on the crystallinity and pore structure of the pristine material, therefore the modification is still accessible for the accommodation of guest species.

We subsequently incorporated linear polymers into the perfluorinated sulfonic acid containing frameworks, aiming to alter the local environment of the acid sites on the COFs. The

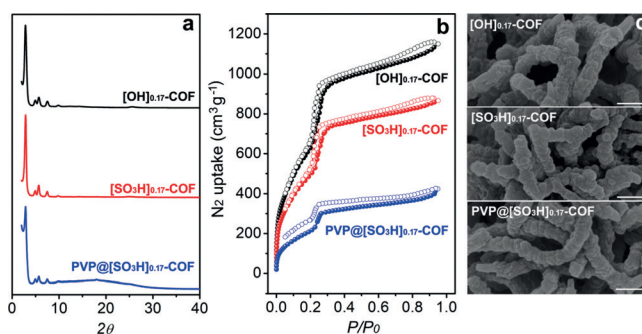


**Figure 2.** a) PXRD patterns, b) N<sub>2</sub> sorption isotherms, and c) SEM images. Scale bar: 500 nm.

reaction medium is an important variable to control the reactivity and selectivity of the catalytic processes; it affects reaction kinetics, product selectivity, the stability of the desired products, together with the economics of downstream separations. We therefore chose 1-vinyl-2-pyrrolidone as a representative monomer in a proof-of-principle study. Our choice is also based on the following considerations: 1) The corresponding polymer, polyvinylpyrrolidone (PVP), is the polymeric analogue of 1-methyl-2-pyrrolidinone (NMP), which is a ubiquitous solvent in organic transformations. 2) Due to the high boiling point of 1-methyl-2-pyrrolidone, isolating products from this solvent is cumbersome and even worse, side reactions often accompany the separation process. We envisioned that the unbound PVP chains could provide a similar solvation environment as NMP in the reaction, thereby regulating the catalytic performance, while the heterogeneous nature of the composites would enable ready product isolation.

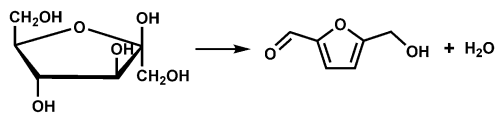
To accommodate the PVP polymers in the COF pore channels, in situ polymerization of 1-vinyl-2-pyrrolidone monomer in  $[\text{SO}_3\text{H}]_x$ -COFs was performed at 80 °C for 3 days. The resulting product was washed thoroughly with DMF to remove unincorporated polymers and unreacted monomers, affording the material denoted as PVP@[ $\text{SO}_3\text{H}$ ]<sub>x</sub>-COFs. The appearance of C=O stretching vibrations (1670 cm<sup>-1</sup>) in the FTIR spectrum corresponding to the amide bond in the pyrrolidinone moiety provided evidence for the incorporation of PVP (Figure S6). The emergence of peaks at 175.9 ppm as well as in the range of 17.4–45.6 ppm in the <sup>13</sup>C MAS NMR spectrum attributable to the polymerized 1-vinyl-2-pyrrolidone moieties confirmed the polymers' encapsulation (Figure S7). To provide additional chemical characterization, the PVP polymers within PVP@[ $\text{SO}_3\text{H}$ ]<sub>0.17</sub>-COF were isolated from the host for <sup>1</sup>H NMR spectroscopy. The spectrum mirrors that of the commercial PVP, specifically lacking peaks between 5.5–7.0 ppm corresponding to the vinylic hydrogen peaks of the monomer (Figure S8). Gel permeation chromatography (GPC) analyses gave an average molecular weight (Mw) of 5833 g mol<sup>-1</sup>, showing proof that the isolated PVP consist of up to 53 monomeric units (Figure S9).

To gain a better understanding of the entrapment of the polymer within  $[\text{SO}_3\text{H}]_{0.17}$ -COF, scanning electron microscopy (SEM) images were collected. The changes in morphology were indistinguishable, indicating that the polymer is included within the pores of the COF and not on the surface (Figure 2c). To quantify how much of the PVP polymer is present within the composite, elemental analysis was performed, and the PVP content was determined to be 33 wt % (Table S1). We then examined the structural integrity of the composite. The crystallinity of the COF was maintained as evidenced by PXRD. The decrease in the relative diffraction intensity can be explained by the change in the electron density of  $[\text{SO}_3\text{H}]_{0.17}$ -COF after it was filled with PVP (Figure 2a). As expected, a decrease in BET surface area from 1510 m<sup>2</sup> g<sup>-1</sup> for  $[\text{SO}_3\text{H}]_{0.17}$ -COF to 644 m<sup>2</sup> g<sup>-1</sup> for PVP@[ $\text{SO}_3\text{H}$ ]<sub>0.17</sub>-COF was observed, yet the reactants are still able to reach the active sites situated on the pore surfaces (Figure 2b). The <sup>31</sup>P MAS NMR spectrum of TMPO after association with PVP@-

$[\text{SO}_3\text{H}]_{0.17}$ -COF showed a singlet peak at 75.6 ppm, a value comparable to that of TMPO interacting with  $[\text{SO}_3\text{H}]_{0.17}$ -COF (76.0 ppm), indicative of the maintenance of acid strength after the incorporation of PVP (Figure S4).

To demonstrate the possibility of the incorporated PVP as an alternative to NMP in regulating the performance of the acid sites, we set out to evaluate the performance PVP@[ $\text{SO}_3\text{H}$ ]<sub>0.17</sub>-COF of in the selective dehydration of fructose to produce HMF, a transformation bridging biomass chemistry and petrochemistry.<sup>[14]</sup> An important factor in the synthesis of HMF through sugar dehydration is the occurrence of side products, including organic acids and humins (Figure S10). Although, the formation of those disfavored products can be suppressed by performing the reaction in solvents like NMP, it remains a substantial challenge to isolate HMF in an energy-friendly manner from this high-boiling-point solvent.<sup>[15]</sup> To give a better illustration, PVP@[ $\text{SO}_3\text{H}$ ]<sub>0.17</sub>-COF was benchmarked against other acid catalysts (Nafion NR50, Amberlyst-15, and 4-methylbenzenesulfonic acid (TsOH)) for HMF selectivity and output efficiency using THF as a reaction medium. The advantages of using THF as the solvent are that it allows for ready product isolation and negates the need to purify HMF from unreacted fructose due to its negligible solubility at room temperature. Our benchmark materials were chosen based on their well-proven efficiency for this transformation in the presence of NMP (Table S3), and their catalytic activities were evaluated with respect to the number of active sites of the catalyst. PVP@[ $\text{SO}_3\text{H}$ ]<sub>0.17</sub>-COF was found to be very efficient in a wide range of temperatures. The HMF selectivity of this composite was 99.1 % at 100 °C and lower, yet remained at 92.8 % at 140 °C (Table S4). A full fructose conversion and a HMF yield of 99.1 % were achieved for PVP@[ $\text{SO}_3\text{H}$ ]<sub>0.17</sub>-COF within 30 min, which compares far more favorably to the corresponding values of  $[\text{SO}_3\text{H}]_{0.17}$ -COF, as well as Nafion NR50, Amberlyst-15, and TsOH, affording fructose conversions of 23.2 %, 9.7 %, 15.3 %, and 28.5 % as well as HMF yields of 17.9 %, 5.3 %, 10.3 %, and 20.9 %, respectively, under otherwise identical conditions. Prolonging the reaction time did not afford satisfied results, demonstrating the importance of the PVP polymer (Table 1). Given the undetected HMF rehydration products, levulinic acid and formic acid, we reason that the decreased HMF selectivity along with the reaction is a result of cross-polymerization between HMF and fructose (see details in Figure S11).

To confirm the role of pyrrolidone moieties, we carried out a series of control experiments. Adding free NMP to those catalytic systems allowed catalytic activity to be restored. Yet it was not comparable to that of PVP@[ $\text{SO}_3\text{H}$ ]<sub>0.17</sub>-COF, even when there were more pyrrolidone moieties than in PVP@[ $\text{SO}_3\text{H}$ ]<sub>0.17</sub>-COF. This is probably because the complementary catalytic partner is diluted in the liquid phase, which does not permit the full pairing of all the active components (Table S5). Adding PVP did not yield an appreciable improvement in activity of the solid catalysts; however, significantly accelerated activity could be measured with TsOH. This can be explained by the fact that the PVP polymer chains coiled, preventing it from fully approaching the active sites, thereby leading to ineffectual cooperation (Table S5). In contrast, the

**Table 1:** Data for the dehydration of fructose to HMF over various catalysts using THF as the solvent.<sup>[a]</sup>

Entry	Catalyst	<i>t</i> [min]	Conv. [%]	Sel. [%] <sup>[b]</sup>	Yield [%] <sup>[b]</sup>
1 <sup>[c]</sup>	PVP@[SO <sub>3</sub> H] <sub>0.17</sub> -COF	30	> 99.5	99.1	99.1
2	[SO <sub>3</sub> H] <sub>0.17</sub> -COF	30	23.2	77.1	17.9
		(120)	(94.6)	(35.2)	(33.3)
3	Nafion NR50	30	9.7	54.6	5.3
		(360)	(89.3)	(19.4)	(17.3)
4	Amberlyst-T5	30	15.3	67.1	10.3
		(180)	(95.2)	(29.5)	(28.1)
5	TsOH	30	28.5	73.5	20.9
		(120)	(> 99.5)	(37.8)	(37.8)
6	PVP&DVB@[SO <sub>3</sub> H] <sub>0.17</sub> -COF	30	86.7	62.7	54.9
7	PVP@[SO <sub>3</sub> H] <sub>0.33</sub> -COF	30	96.4	89.3	86.1
8	PVP@[SO <sub>3</sub> H] <sub>0.50</sub> -COF	30	91.2	75.6	68.9
9 <sup>[d]</sup>	PVP@[SO <sub>3</sub> H] <sub>0.17</sub> -COF	30	> 99.5	97.1	97.1
10 <sup>[e]</sup>	PVP@[SO <sub>3</sub> H] <sub>0.17</sub> -COF	30	> 99.5	98.2	98.2

[a] Reaction conditions: fructose (100 mg, 0.56 mmol), catalyst (based on the amount of sulfonic acid 2.0 mol %), 100 °C, THF (3.0 mL), and optimized reaction time. [b] HMF selectivity and yield were determined by the combination of liquid chromatography and gas chromatography.

[c] Yield of isolated HMF: 94.5% (Figure S12). [d] Recycled five times.

[e] Fructose (1.0 g), PVP@[SO<sub>3</sub>H]<sub>0.17</sub>-COF (2.0 mol %), 100 °C, and THF (20 mL) for 30 min. The values in parentheses refer to reaction time and corresponding conversion of fructose and selectivity and yield of HMF at that point.

molecular catalyst TsOH is easily diffused to the nearby pyrrolidone moieties in PVP, allowing for cooperation. This also indicates the superiority of *in situ* polymerization, which renders the polymers trapped within the pores for maximum utilization.

The results above imply that the local concentration of the pyrrolidone moieties has a great effect on the performance of the acid sites. To prove this, we synthesized PVP@[SO<sub>3</sub>H]<sub>0.33</sub>-COF and PVP@[SO<sub>3</sub>H]<sub>0.50</sub>-COF with PVP amounts similar to that in PVP@[SO<sub>3</sub>H]<sub>0.17</sub>-COF (Figures S13–S20). Catalytic data revealed that upon increasing the density of sulfonic acid groups in the COFs, diminished productivity as well as selectivity to HMF was observed from 99.1% to 86.1% and 68.9% for PVP@[SO<sub>3</sub>H]<sub>0.17</sub>-COF, PVP@[SO<sub>3</sub>H]<sub>0.33</sub>-COF, and PVP@[SO<sub>3</sub>H]<sub>0.50</sub>-COF, with initial reaction rates of 0.024, 0.018, and 0.013 mmol min<sup>-1</sup>, respectively (Table 1, entries 1, 7, and 8; for detailed experimental procedures, see the Supporting Information). It was thus deduced that the ratio of pyrrolidone to the -SO<sub>3</sub>H group content is vital to the performance. In line with the highest average pyrrolidone moiety density per -SO<sub>3</sub>H group, among the samples tested, PVP@[SO<sub>3</sub>H]<sub>0.17</sub>-COF exhibited the highest HMF yield, ranking it among the best catalytic systems reported thus far as well as surpassing those using NMP as a solvent (Table S6).

To gain insight about how the cooperation occurs between the threaded PVP and the acid sites appended on the COFs, we reasoned that the flexibility of the linear polymer should

play an important role. To give experimental evidence, a composite with less flexibility was synthesized. In this case, the PVP chains threaded through the channels of the COF are locked in place by introduction of a covalent cross-linker (divinylbenzene, DVB) during the polymerization process. The resulting catalyst (PVP&DVB@[SO<sub>3</sub>H]<sub>0.17</sub>-COF, BET: 599 m<sup>2</sup> g<sup>-1</sup>, Figure S21) afforded a HMF yield of 64.9%, around 60% as much achieved by employing PVP@[SO<sub>3</sub>H]<sub>0.17</sub>-COF, suggesting that the restricted flexibility of cross-linked PVP significantly reduces the catalytic components' cooperation. In previous studies of reactions involving carbohydrates, some favorable intermediates identified are complexes that incorporate the solvent moieties as a result of the strong solvation effect due to hydrogen-bonding interactions; these intermediates favor the subsequent desired transformation.<sup>[15]</sup> Therefore, we infer that the flexible PVP chains act as a pseudo-solvent, encapsulating reactants in a local microenvironment by the hydrogen-bonding interactions between C=O and the hydroxyl protons of fructose, as evidenced by PXRD and IR analyses (Figures S22 and S23). Based on our findings and previous research, a tentative mechanism is proposed for the dehydration of fructose to HMF catalyzed by PVP@[SO<sub>3</sub>H]<sub>0.17</sub>-SO<sub>3</sub>H (Figure S24).<sup>[16]</sup>

To examine the stability as well as recyclability of the catalytic material, PVP@[SO<sub>3</sub>H]<sub>0.17</sub>-COF was used as a catalyst up to five times. As depicted in Figure S25, HMF was obtained in 97.1% yield even after five runs and no significant loss of activity was observed. A hot filtration test revealed that the obtained activity is not related to any leaching of the catalytically active acid sites (no remaining activity in the supernatant). The neutrality of the isolated product further confirmed that no undesired leaching processes of acid species had occurred during the course of the catalytic transformation. The catalytic system was also applicable for a larger scale reaction, where 1.0 g of fructose was successfully converted into HMF, which can be readily isolated after simple filtration of the catalyst and evaporation of THF (see <sup>1</sup>H NMR spectrum in Figure S26). The structural integrity of PVP@[SO<sub>3</sub>H]<sub>0.17</sub>-COF was also retained after the reactions, as confirmed by PXRD analysis of the spent catalyst (Figure S27).

Advantageously, our strategy of inserting linear polymers to promote reaction performance is also easily extended to other functional materials. To showcase this, we incorporated an ionic polymer (PIL; for details see the experimental section in the Supporting Information) within the COFs and subjected them to identical reaction procedures. PIL@[SO<sub>3</sub>H]<sub>0.17</sub>-COF also demonstrated a remarkably improved efficiency of 97.6% HMF yield within 30 min at 100 °C in the presence of THF.

Our synthetic approach overcomes the challenges of the spatial isolation of catalytic elements. We have provided a rigorous experimental demonstration that multiple non-covalent substrate–catalyst interactions can be integrated to regulate the reaction outcomes of heterogeneous catalysts. The benefits of both molecular and solid materials are leveraged such that the flexible linear polymer chains confined in the pore channels cooperate with the active sites anchored on the COF pore walls. In this way, the

catalytic potential is fully exploited, while the catalyst is also recyclable. This approach should be relevant for parallel and more complex reaction schemes, ultimately facilitating the development of new catalytic processes. Together with its high versatility to integrate with other functional materials, we envisage our strategy presented herein as a cornerstone to realize a new paradigm in the design of multifunctional molecular assemblies to control functions at a level approaching that of biological systems.

## Acknowledgements

We acknowledge the National Science Foundation of China (21720102001 and 91634201) as well as the National Science Foundation (DMR-1352065) and the University of South Florida for financial support of this work. We also extend our appreciation to the Distinguished Scientist Fellowship Program (DSFP) at King Saud University for funding this work partially.

## Conflict of interest

The authors declare no conflict of interest.

**Keywords:** acid catalysis · biomass · covalent organic frameworks · host–guest systems · solvation

**How to cite:** *Angew. Chem. Int. Ed.* **2019**, *58*, 8670–8675  
*Angew. Chem.* **2019**, *131*, 8762–8767

- [1] a) S. A. Cook, A. S. Borovik, *Acc. Chem. Res.* **2015**, *48*, 2407–2414; b) M. Raynal, P. Ballester, A. Vidal-Ferran, P. W. N. M. van Leeuwen, *Chem. Soc. Rev.* **2014**, *43*, 1734–1787.
- [2] a) A. J. Neel, M. J. Hilton, M. S. Sigman, F. D. Toste, *Nature* **2017**, *543*, 637–646; b) F. D. Toste, M. S. Sigman, S. J. Miller, *Acc. Chem. Res.* **2017**, *50*, 609–615; c) L. Liu, T.-Y. Zhou, S. G. Telfer, *J. Am. Chem. Soc.* **2017**, *139*, 13936–13943; d) M. Zhao, K. Yuan, Y. Wang, G. Li, J. Guo, L. Gu, W. Hu, H. Zhao, Z. Tang, *Nature* **2016**, *539*, 76–80.
- [3] a) J. Meeuwissen, J. N. H. Reek, *Nat. Chem.* **2010**, *2*, 615–621; b) N. A. Grosso-Giordano, C. Schroeder, A. Okrut, A. Solovoyov, C. Schöttle, W. Chassé, N. Marinković, H. Koller, S. I. Zones, A. Katz, *J. Am. Chem. Soc.* **2018**, *140*, 4956–4960.
- [4] a) A. P. Côté, A. I. Benin, N. W. Ockwig, M. O’Keeffe, A. J. Matzger, O. M. Yaghi, *Science* **2005**, *310*, 1166–1170; b) X. Feng, X. Ding, D. Jiang, *Chem. Soc. Rev.* **2012**, *41*, 6010–6022; c) S.-Y. Ding, W. Wang, *Chem. Soc. Rev.* **2013**, *42*, 548–568; d) Y. Jin, Y. Hu, W. Zhang, *Nat. Rev. Chem.* **2017**, *1*, s41570-017; e) R. P. Bisbey, W. R. Dichtel, *ACS Cent. Sci.* **2017**, *3*, 533–543; f) F. Beuerle, B. Gole, *Angew. Chem. Int. Ed.* **2018**, *57*, 4850–4878; *Angew. Chem.* **2018**, *130*, 4942–4972; g) Y. Song, Q. Sun, B. Aguila, S. Ma, *Adv. Sci.* **2019**, *6*, 1801410; h) Y. Lan, X. Han, M. Tong, H. Huang, Q. Yang, D. Liu, X. Zhao, C. Zhong, *Nat. Commun.* **2018**, *9*, 5274; i) S. Kandambeth, K. Dey, R. Banerjee, *J. Am. Chem. Soc.* **2019**, *141*, 1807–1822.
- [5] a) M. Calik, F. Auras, L. M. Salonen, K. Bader, I. Grill, M. Handloser, D. D. Medina, M. Dogru, F. Löbermann, D. Trauner, A. Hartschuh, T. Bein, *J. Am. Chem. Soc.* **2014**, *136*, 17802–17807; b) Y. Du, H. Yang, J. M. Whiteley, S. Wan, Y. Jin, S.-H. Lee, W. Zhang, *Angew. Chem. Int. Ed.* **2016**, *55*, 1737–1741; *Angew. Chem.* **2016**, *128*, 1769–1773; c) S. Wang, Q. Wang, P. Shao, Y. Han, X. Gao, L. Ma, S. Yuan, X. Ma, J. Zhou, X. Feng, B. Wang, *J. Am. Chem. Soc.* **2017**, *139*, 4258–4261.
- [6] a) S.-Y. Ding, J. Gao, Q. Wang, Y. Zhang, W.-G. Song, C.-Y. Su, W. Wang, *J. Am. Chem. Soc.* **2011**, *133*, 19816–19822; b) X. Wang, X. Han, J. Zhang, X. Wu, Y. Liu, Y. Cui, *J. Am. Chem. Soc.* **2016**, *138*, 12332–12335; c) V. S. Vyas, F. Haase, L. Stegbauer, G. Savasci, F. Podjaski, C. Ochsenfeld, B. V. Lotsch, *Nat. Commun.* **2015**, *6*, 8508; d) P. Pachfule, A. Acharjya, J. Roeser, T. Langenhahn, M. Schwarze, R. Schomäcker, A. Thomas, J. Schmidt, *J. Am. Chem. Soc.* **2018**, *140*, 1423–1427; e) H. Liu, J. Chu, Z. Yin, X. Cai, L. Zhuang, H. Deng, *Chem* **2018**, *4*, 1696–1709; f) Q. Fang, S. Gu, J. Zeng, Z. Zhuang, S. Qiu, Y. Yan, *Angew. Chem. Int. Ed.* **2014**, *53*, 2878–2882; *Angew. Chem.* **2014**, *126*, 2922–2926; g) Y. Peng, Z. Hu, Y. Gao, D. Yuan, Z. Kang, Y. Qian, N. Yan, D. Zhao, *ChemSusChem* **2015**, *8*, 3208.
- [7] a) Q. Sun, C.-W. Fu, B. Aguila, J. A. Perman, S. Wang, H.-Y. Huang, F.-S. Xiao, S. Ma, *J. Am. Chem. Soc.* **2018**, *140*, 984–992; b) H. Ma, B. Liu, B. Li, L. Zhang, Y.-G. Li, H.-Q. Tan, H.-Y. Zang, G. Zhu, *J. Am. Chem. Soc.* **2016**, *138*, 5897–5903; c) C. R. Mulzer, L. Shen, R. P. Bisbey, J. R. McKone, N. Zhang, H. D. Abruña, W. R. Dichtel, *ACS Cent. Sci.* **2016**, *2*, 667–673.
- [8] a) Q. Sun, B. Aguila, J. A. Perman, N. Nguyen, S. Ma, *J. Am. Chem. Soc.* **2016**, *138*, 15790–15796; b) B. Aguila, Q. Sun, X. Wang, E. O’Rourke, A. M. Al-Enizi, A. Nafady, S. Ma, *Angew. Chem. Int. Ed.* **2018**, *57*, 10107–10111; *Angew. Chem.* **2018**, *130*, 10264–10268; c) L. Bromberg, X. Su, T. A. Hatton, *Chem. Mater.* **2014**, *26*, 6257–6264.
- [9] a) C. Reichardt, T. Welton, *Solvents and solvent effects in organic chemistry*, 2nd ed., VCH Publishers, Weinheim, **1988**; b) G. Balakrishnan, S. K. Sahoo, B. K. Chowdhury, S. Umapathy, *Faraday Discuss.* **2010**, *145*, 443–466.
- [10] a) H. Xu, J. Gao, D. Jiang, *Nat. Chem.* **2015**, *7*, 905–912; b) H. Xu, S. Tao, D. Jiang, *Nat. Mater.* **2016**, *15*, 722–726.
- [11] a) X. Zhang, Y. Zhao, S. Xu, Y. Yang, J. Liu, Y. Wei, Q. Yang, *Nat. Commun.* **2014**, *5*, 3170; b) K. Nakajima, M. Hara, *ACS Catal.* **2012**, *2*, 1296–1304.
- [12] Q. Sun, K. Hu, K. Leng, X. Yi, B. Aguila, Y. Sun, A. Zheng, X. Meng, S. Ma, F.-S. Xiao, *J. Mater. Chem. A* **2018**, *6*, 18712–18719.
- [13] A. Zheng, H. Zhang, X. Lu, S.-B. Liu, F. Deng, *J. Phys. Chem. B* **2008**, *112*, 4496–4505.
- [14] a) Y. Román-Leshkov, J. N. Chheda, J. A. Dumesic, *Science* **2006**, *312*, 1933–1937; b) R. Alamillo, A. J. Crisci, J. M. R. Gallo, S. L. Scott, J. A. Dumesic, *Angew. Chem. Int. Ed.* **2013**, *52*, 10349–10351; *Angew. Chem.* **2013**, *125*, 10539–10541; c) G. Yong, Y. Zhang, J. Y. Ying, *Angew. Chem. Int. Ed.* **2008**, *47*, 9345–9348; *Angew. Chem.* **2008**, *120*, 9485–9488; d) H. Zhao, J. E. Holladay, H. Brown, Z. C. Zhang, *Science* **2007**, *316*, 1597–1600; e) G.-H. Wang, J. Hilgert, F. H. Richter, F. Wang, H.-J. Bongard, B. Spliethoff, C. Weidenthaler, F. Schüth, *Nat. Mater.* **2014**, *13*, 293–300; f) Q. Xia, Z. Chen, Y. Shao, X. Gong, H. Wang, X. Liu, S. F. Parker, X. Han, S. Yang, Y. Wang, *Nat. Commun.* **2016**, *7*, 11162; g) Q. Sun, S. Wang, B. Aguila, X. Meng, S. Ma, F.-S. Xiao, *Nat. Commun.* **2018**, *9*, 3236.
- [15] a) L.-K. Ren, L.-F. Zhu, T. Qi, J.-Q. Tang, H.-Q. Yang, C.-W. Hu, *ACS Catal.* **2017**, *7*, 2199–2212; b) A. Corma, S. Iborra, A. Velty, *Chem. Rev.* **2007**, *107*, 2411–2502; c) M. E. Zakrzewska, E. Bogel-Lukasik, R. Bogel-Lukasik, *Chem. Rev.* **2011**, *111*, 397–417; d) C. J. Clarke, W.-C. Tu, O. Levers, A. Bröhl, J. P. Hallett, *Chem. Rev.* **2018**, *118*, 747–800.
- [16] T. W. Walker, A. K. Chew, H. Li, B. Demir, Z. C. Zhang, G. W. Huber, R. C. Van Lehn, J. A. Dumesic, *Energy Environ. Sci.* **2018**, *11*, 617–628.

Manuscript received: January 2, 2019

Revised manuscript received: February 21, 2019

Accepted manuscript online: April 7, 2019

Version of record online: April 25, 2019